ORIGINAL RESEARCH

Predictive Value of ^{18}F-Sodium Fluoride Positron Emission Tomography in Detecting High-Risk Coronary Artery Disease in Combination With Computed Tomography

Toshiro Kitagawa, MD, PhD; Hideya Yamamoto, MD, PhD; Yumiko Nakamoto, MD; Ko Sasaki, RT; Shinya Toshimitsu, RT; Fuminari Tatsugami, MD, PhD; Kazuo Awai, MD, PhD; Yutaka Hirokawa, MD, PhD; Yasuki Kihara, MD, PhD

Background—Application of ^{18}F-sodium fluoride (^{18}F-NaF) positron emission tomography (PET) to coronary artery disease has attracted interest. We investigated the utility of ^{18}F-NaF uptake for predicting coronary events and evaluated the combined use of coronary computed tomography (CT) angiography (CCTA) and ^{18}F-NaF PET/CT in coronary artery disease risk assessment.

Methods and Results—This study included patients with ≥1 coronary atherosclerotic lesion detected on CCTA who underwent ^{18}F-NaF PET/CT. High-risk plaque on CCTA was defined as plaque with low density (<30 Hounsfield units) and high remodeling index (>1.1). Focal ^{18}F-NaF uptake in each lesion was quantified using the maximum tissue:background ratio (TBR_{max}), and maximum TBR_{max} per patient (M-TBR_{max}) was determined. Thirty-two patients having a total of 112 analyzed lesions were followed for 2 years after ^{18}F-NaF PET/CT scan, and 11 experienced coronary events (acute coronary syndrome and/or late coronary revascularization [after 3 months]). Patients with coronary events had higher M-TBR_{max} than those without (1.39±0.18 versus 1.19±0.17, respectively; P=0.0034). The optimal M-TBR_{max} cutoff to predict coronary events was 1.28 (area under curve: 0.79). Patients with M-TBR_{max} ≥1.28 had a higher risk of earlier coronary events than those with lower M-TBR_{max} (P=0.0062 by log-rank test). In patient-based (n=41) and lesion-based (n=143) analyses of CCTA findings that predicted higher coronary ^{18}F-NaF uptake, the presence of high-risk plaque was a significant predictor of both M-TBR_{max} ≥1.28 and TBR_{max} ≥1.28.

Conclusions—^{18}F-NaF PET/CT has the potential to detect high-risk coronary artery disease and individual coronary lesions and to predict future coronary events when combined with CCTA.

Clinical Trial Registration—URL: www.umin.ac.jp. Unique identifier: UMIN000013735. **(*J Am Heart Assoc*. 2018;7:e010224. DOI: 10.1161/JAHA.118.010224.)**

Key Words: coronary artery disease • coronary atherosclerosis • coronary computed tomography angiography • coronary event • positron emission tomography • sodium fluoride

The clinical utility of ^{18}F-sodium fluoride (^{18}F-NaF) positron emission tomography (PET) has recently attracted interest in the field of cardiovascular medicine. Use of the technique to evaluate coronary arteries, major arteries, and aortic valves has been reported.[1-3] The ^{18}F-NaF tracer reacts with hydroxyapatite, which is the central component of vascular calcification and is laid down during the earliest and most active stages of mineralization. An association between osteogenesis and inflammation has been suggested in the development of atheroslcerosis.[4,5] Interestingly, a correlation has been reported between ^{18}F-NaF uptake in coronary arteries and thoracic fat, which is considered a marker of inflammation and atherosclerotic cardiovascular risk.[6] Thus, ^{18}F-NaF PET may provide a novel strategy to biologically assess the risk of coronary atherosclerosis.

From the Department of Cardiovascular Medicine, Hiroshima University Graduate School of Biomedical and Health Sciences, Hiroshima, Japan (T.K., H.Y., Y.N., Y.K.); Hiroshima Heiwa Clinic, Hiroshima, Japan (K.S., S.T., Y.H.); Department of Diagnostic Radiology, Hiroshima University Hospital, Hiroshima, Japan (F.T., K.A.).

Accompanying Tables S1 and S2 are available at https://www.ahajournals.org/doi/suppl/10.1161/JAHA.118.010224

Correspondence to: Toshiro Kitagawa, MD, PhD, Department of Cardiovascular Medicine, Hiroshima University Graduate School of Biomedical & Health Sciences, 1-2-3 Kasumi, Minami-Ku, Hiroshima 734-8551, Japan. E-mail: toshirok@hiroshima-u.ac.jp

Received June 28, 2018; accepted August 29, 2018.

Clinical Perspective

What Is New?

- Higher ^{18}F-sodium fluoride uptake in coronary atherosclerotic lesions on positron emission tomography had a predictive value for 2-year coronary events (acute coronary syndrome and/or late coronary revascularization [after 3 months]) that was superior to the findings on coronary computed tomography angiography.
- The presence of high-risk plaque on coronary computed tomography angiography, defined as plaque with low density and high remodeling index, was a predictor of higher coronary ^{18}F-sodium fluoride uptake in both patient- and lesion-based analyses.

What Are the Clinical Implications?

- ^{18}F-sodium fluoride positron emission tomography/computed tomography has the potential to detect high-risk coronary artery disease and individual coronary lesions and to predict future coronary events when combined with coronary computed tomography angiography.

Coronary computed tomography angiography (CCTA) is a main noninvasive imaging modality in the management of coronary artery disease (CAD). We previously reported the relationship between coronary plaque characteristics on CCTA and ^{18}F-NaF uptake on PET.[7] This relationship raises the possibility of developing a step-by-step approach to identify high-risk patients and coronary atherosclerotic lesions with CCTA and ^{18}F-NaF PET/computed tomography (PET/CT) in clinical practice. However, information on the value of ^{18}F-NaF PET/CT for CAD risk assessment is limited, and its prognostic value in predicting coronary events has not been evaluated. Intense ^{18}F-NaF uptake localizes preferentially in culprit lesions of patients suffering from acute myocardial infarction (MI)[8]; however, no evidence to date shows the prognostic significance of ^{18}F-NaF signals.

The aims of this study were to investigate the utility of ^{18}F-NaF uptake for predicting coronary events and to evaluate the effective combined use of CCTA and ^{18}F-NaF PET/CT in CAD risk assessment.

Methods

The data, analytic methods, and study materials will not be made available to other researchers for the purpose of reproducing the results or replicating the procedure.

This study consisted of 2 parts. First, we compared the prognostic value of ^{18}F-NaF PET/CT versus CCTA for the prediction of future coronary events. Next, to develop a step-by-step approach using CCTA and ^{18}F-NaF PET/CT, we evaluated how patient- and lesion-based CCTA findings related to ^{18}F-NaF uptake. Our hospital's ethics committee approved the study protocol; written informed consent was obtained from all patients. The protocol has been published in the Japan UMIN Clinical Trials Registry (identifier: UMIN000013735).

Patients

We prospectively recruited consecutive patients with known or suspected CAD who underwent both cardiac CT and ^{18}F-NaF PET/CT between June 2014 and December 2017. All patients were referred for cardiac CT as a first step for the investigation and diagnosis of CAD. To be included in the ^{18}F-NaF PET/CT study as a second step, patients had to have at least 1 coronary atherosclerotic lesion detected on CCTA in segments >2-mm in diameter according to the Society of Cardiovascular Computed Tomography's 18-segment model[9] and needed to agree to study participation. Exclusion criteria included the presence of cardiac arrhythmias (ie, atrial fibrillation, frequent paroxysmal premature beats), contraindications to iodinated contrast medium, unstable hemodynamic conditions, and ongoing MI or unstable angina (UA). Patients receiving dialysis, which would have been a potentially confounding factor in the analysis of coronary calcification, were also excluded. We collected clinical information, including coronary risk factors and a past history of MI or UA. History of MI or UA was determined as explained in our previous report.[7]

Image Acquisition and Analysis of CCTA (First Step)

All patients underwent cardiac CT with a 320-detector row CT scanner (Aquilion ONE; Canon Medical Systems), as described in our previous report.[7] Briefly, a plain scan was taken to measure coronary calcium score (CCS) according to the Agatston method (slice thickness: 3.0 mm; maximum tube current: 270 mA; tube voltage: 120 kV). We acquired data sets for CCTA with the HeartNAVI system (collimation, 320×0.5 mm; tube current, 350–580 mA; tube voltage, 120 kV; Canon Medical Systems) with retrospective ECG gating. All reconstructed CT image data were transferred to an offline workstation (Advantage Workstation v4.2; GE Healthcare) for postprocessing and image analysis. The mean effective radiation dose according to the dose–length product was 8 mSv per patient, as in our previous study using the same scanner.[10]

Two blinded independent observers evaluated the coronary lumen for stenosis and the presence of atherosclerotic lesions in all coronary segments >2 mm in diameter on CCTA. The severity of stenosis was quantified by visual estimation into 5 categories (0%, 1–24%, 25–49%, 50–69%, and ≥70% stenosis).[9]

Lumen stenosis ≥70% in any vessel or ≥50% in the left main coronary artery was considered clinically obstructive. Coronary atherosclerotic lesions were divided into 1 of 3 plaque types[7,9]: *calcified plaque*, defined as a structure on the vessel wall with CT density entirely above that of the contrast-enhanced coronary lumen or >130 Hounsfield units; *noncalcified plaque*, defined as an entirely low-density mass >1 mm^2, located within the vessel wall and clearly distinguishable from the contrast-enhanced coronary lumen and surrounding pericardial tissue; and *partially calcified plaque* (PCP), defined as a mass containing both calcified and noncalcified plaque components. For noncalcified plaque and PCP, each noncalcified component was evaluated for its minimum CT density and vascular remodeling index, as in our previous studies.[11,12] *High-risk plaque* (HRP) was defined as noncalcified plaque or PCP with a low density (<30 Hounsfield units) and a high remodeling index (>1.1), which are high-risk characteristics resulting in acute coronary syndrome (ACS).[13,14]

If the initial assessments of coronary stenosis, plaque type, and HRP differed between the 2 independent observers, agreement was reached by consensus.

Image Acquisition and Analysis of ^{18}F-NaF PET/CT (Second Step)

Within 1 month after cardiac CT imaging, all patients underwent combined PET/CT imaging with a hybrid scanner (Discovery ST Elite-Performance, GE Healthcare), as in our previous report.[7] Briefly, after administration of ^{18}F-NaF (target dose: 370 MBq) and a subsequent 60-minute rest, a nonenhanced CT scan for attenuation correction and an ECG-gated emission PET scan of the thorax (25-minute acquisition using the 3-dimensional mode) were performed. Then an ECG-gated CT scan for fusion with PET images was performed with the same axial coverage (collimation: 16×0.625 mm; tube current: 250 mA; tube voltage: 120 kV). The PET component of the combined imaging system allows simultaneous acquisition of 47 transaxial PET images with an interslice spacing of 3.27 mm in 1 bed position. The PET data were reconstructed with an ordered-subset expectation maximization–based iterative reconstruction algorithm called VUE Point Plus (21 subsets and 2 iterations).

The reconstruction of PET data was performed in 8 multiple phases of the cardiac cycle, and the diastolic phase (62.5–75%) was used for analysis. The PET and CT images were fused and analyzed by 2 experienced, blinded readers with an offline workstation (Advantage Workstation v4.4; GE Healthcare). Each coronary atherosclerotic lesion was identified visually using locations of vessel calcium and branches in the previously scanned coronary CT images (noncontrast and CCTA images) as landmarks. For quantification of ^{18}F-NaF uptake, an region of interest was drawn around each lesion on 3.27-mm axial slices just beyond the discernible adventitial border. The maximum standardized uptake value (decay-corrected tissue concentration of the tracer divided by the injected dose per body weight) was measured and divided by an averaged mean standardized uptake value in the blood pool, derived from 5 circular regions of interest positioned in the center of the superior vena cava. This was reported as a maximum tissue:background ratio (TBR_{max}) for a measure of ^{18}F-NaF uptake in each coronary atherosclerotic lesion. When multiple coronary atherosclerotic lesions were identified in a patient, maximum TBR_{max} per patient in any lesion (M-TBR_{max}) was determined for a patient-based analysis.

If the coronary atherosclerotic lesions detected on the previously scanned coronary CT images could not be identified confidently on the fused PET/CT images, such lesions were excluded from the analysis via 2-reader consensus.

Follow-up Study on Coronary Events

We followed the occurrence of coronary events after ^{18}F-NaF PET/CT scan in a subgroup of the entire cohort. We recorded follow-up patient information by reviewing hospital records, performing telephone interviews with patients, and contacting primary physicians. All end points were determined by the consensus of 2 blinded reviewers. We focused on the end points of cardiac death; ACS, including nonfatal MI and UA requiring hospitalization; and late coronary revascularization performed ≥3 months after ^{18}F-NaF PET/CT scan. Cardiac death was defined as death caused by acute MI, ventricular arrhythmia, or cardiogenic shock. The occurrence of MI and UA were determined on the basis of the standard criteria[15,16]; culprit lesions were defined as lesions whose onset was associated with ECG changes or those with the most obstructive luminal narrowing on invasive coronary angiography. Late coronary revascularization was performed based on chest symptoms and/or positive myocardial ischemia findings on stress tests; the culprit lesion was determined by primary physicians blinded to CCTA and PET data, based on obstructive appearance (≥75%) on invasive coronary angiography, and/or impaired coronary fractional flow reserve (≤0.75).

Follow-up was censored at 2 years after ^{18}F-NaF PET/CT scan or at the time of event occurrence.

Statistical Analysis

The CCS is expressed as the median value and interquartile range. Other measurements are expressed as mean±SD. The Student *t* test or Mann–Whitney *U* test was used to compare continuous variables between groups. Categorical variables are reported as numbers or proportions and were compared with the Pearson χ^2 test. M-TBR_{max} was tested with a receiver operator characteristic curve to determine the optimal

M-TBR$_{max}$ for predicting coronary events. Event rates were estimated with Kaplan–Meier curves and compared with a log-rank test. A Cox proportional hazards regression model was used to assess predictors of coronary events. Logistic regressions were used to examine the associations between CCTA findings and higher M-TBR$_{max}$ or TBR$_{max}$. Interobserver variability of measured PET activities was determined by calculating the 95% confidence intervals (CIs) for mean differences. All analyses were performed with JMP 10.0.1 statistical software (SAS Institute). *P* values of <0.05 were considered statistically significant.

Results

Baseline Information

A total of 51 patients undergoing cardiac CT were screened for inclusion in the ^{18}F-NaF PET/CT study. Nine patients declined participation in the study, and 1 had incomplete PET data. The remaining 41 patients were included in this study. The 2-year follow-up to monitor for coronary events was completed for 32 of the 41 patients. Table 1 shows the baseline clinical characteristics of the entire and follow-up cohorts. All characteristics, including the proportion of patients with MI or UA history or coronary stent implantation and level of CCS, were similar between the 2 cohorts.

In all 41 subjects, CCTA visualized a total of 158 coronary atherosclerotic lesions, 15 of which could not be identified on the fused PET/CT images. The reasons for the difficulty in identifying lesions on fused PET/CT images were motion artifact (n=5), overspill of activity from the sternal bone (n=2), and the lower spatial resolution of the fused PET/CT images compared with the coronary CT images (n=8). There were no lesions that were hampered by myocardial signal and excluded. As a result, a total of 143 coronary lesions (mean: 3.5±1.2 per patient; range: 2–7 lesions per patient) were analyzed with both CCTA and ^{18}F-NaF PET/CT in the entire cohort. In the follow-up cohort, 112 lesions (mean: 3.5±1.2 per patient; range: 2–7 lesions per patient) were analyzed. We found good interobserver agreement for maximum standardized uptake value (mean difference: 0.02; 95% CI: −0.02 to 0.05), TBR$_{max}$ (mean difference: 0.01; 95% CI: −0.03 to 0.06), and M-TBR$_{max}$ (mean difference: 0.01; 95% CI, −0.06 to 0.07).

Table 1. Baseline Clinical Characteristics of Entire and Follow-up Study Cohorts

Characteristics	Entire (n=41)	Follow-up (n=32)
Age, y	66±9	66±9
Male sex	33 (80)	26 (81)
BMI, kg/m^2	24±3	24±3
Hypertension	29 (70)	23 (72)
Hyperlipidemia	34 (83)	25 (78)
Diabetes mellitus	21 (51)	17 (53)
Current smoking	18 (44)	13 (41)
Statin use	29 (71)	22 (69)
MI or UA history	18 (44)	14 (44)
Coronary stent implantation	10 (24)	6 (19)
CCS	277 (51–1206) (n=31)	260 (53–1258) (n=26)

CCS is expressed as the median value (interquartile range). Other data are expressed as mean±SD or number (proportion). BMI indicates body mass index; CCS, coronary calcium score; MI, myocardial infarction; UA, unstable angina.

CCTA Findings, ^{18}F-NaF Uptake, and Coronary Events

During the follow-up period, 11 patients (34%) experienced coronary events: 1 had MI, 3 had UA requiring hospitalization, and 7 underwent late coronary revascularization. There was no cardiac death. The number of analyzed coronary lesions per patient was higher among patients with coronary events than among those without such events (4.4±1.4 versus 3.0±0.9 lesions, respectively; *P*=0.0028).

Patients with coronary events were more likely than those without to have at least 1 site with obstructive stenosis on CCTA (82% versus 57% of patients, respectively; *P*=0.16; Figure 1A); however, this difference did not reach significance. The proportion of patients with at least 1 HRP on CCTA was similar between patients with coronary events and those without (73% versus 62% of patients, respectively; *P*=0.54; Figure 1B). In contrast, patients with coronary events had higher M-TBR$_{max}$ on ^{18}F-NaF PET/CT than those without (1.39±0.18 versus 1.19±0.17, respectively; *P*=0.0034). The optimal M-TBR$_{max}$ cutoff to predict coronary events was 1.28 (area under the curve, 0.79), which had sensitivity of 73%, specificity of 76%, positive predictive value of 62%, and negative predictive value of 84% (Figure 1C and 1D). The Kaplan–Meier curves demonstrated that patients with M-TBR$_{max}$ ≥1.28 had a higher risk of earlier coronary events than those with lower values (*P*=0.0062 by log-rank test); however, patients with obstructive stenosis (*P*=0.14) and those with HRP (*P*=0.58) did not (Figure 2). On multivariate Cox proportional analysis adjusted for age, sex, presence of coronary risk factors, and statin use, the presence of obstructive stenosis (hazard ratio: 9.4; 95% CI, 1.5–118.4; *P*=0.014) and M-TBR$_{max}$ ≥1.28 (hazard ratio: 8.2; 95% CI, 1.4–79.2; *P*=0.020) remained significant predictors of the 2-year coronary events (Table S1).

In patients with coronary events, culprit lesions (n=11) were more likely than nonculprit lesions (n=37) to have obstructive stenosis (64% versus 32% of lesions, respectively;

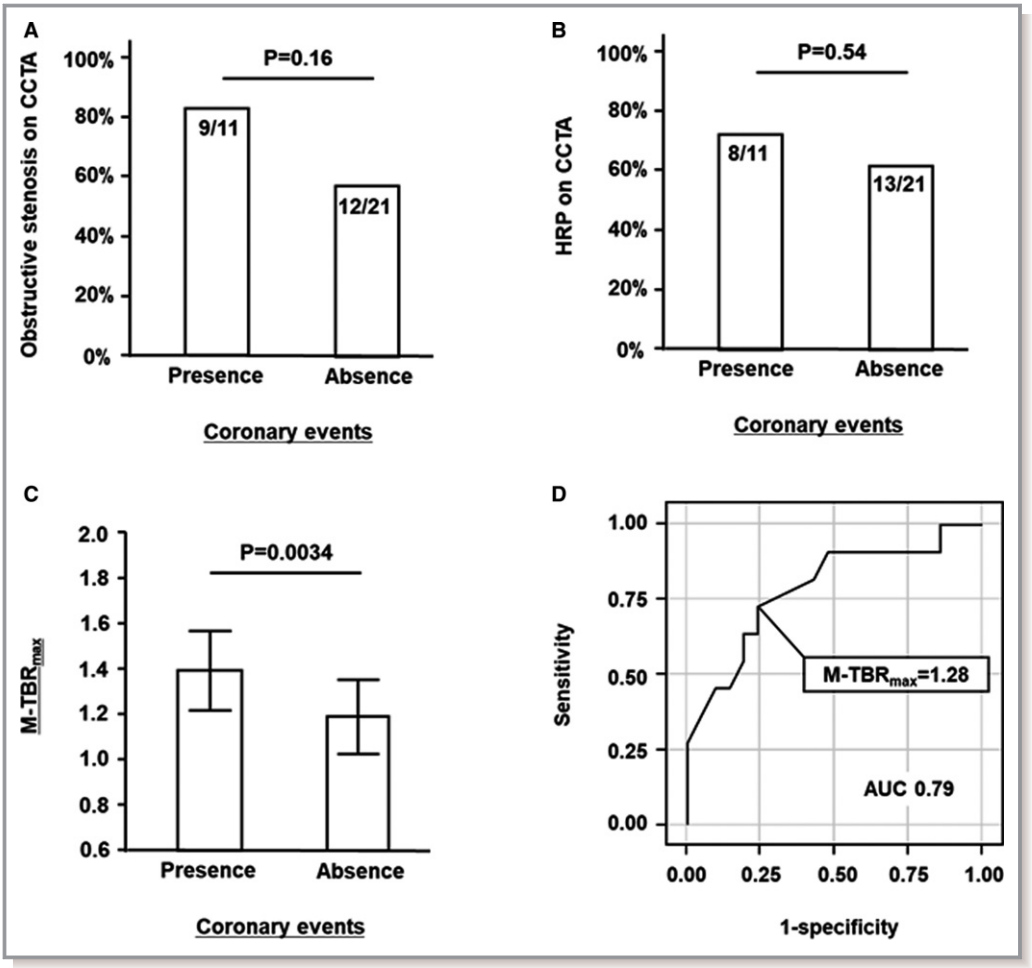

Figure 1. Prevalence of obstructive stenosis (A) and HRP (B) on CCTA, patient-based ^{18}F-sodium fluoride TBR_{max} in patients with vs without coronary events (C), and receiver operating characteristic curve of patient-based TBR_{max} for predicting coronary events (D). There was no significant difference in prevalence of obstructive stenosis or HRP between the groups (A and B). Maximum TBR_{max} per patient (M-TBR_{max}) was higher among patients with coronary events (C); the optimal M-TBR_{max} cutoff to predict coronary events was 1.28 (D). AUC indicates area under the curve; CCTA, coronary computed tomography angiography; HRP, high-risk plaque; TBR_{max}, maximum tissue:background ratio.

P=0.063) and HRP (55% versus 11% of lesions, respectively; *P*=0.0017) on CCTA and had a higher TBR_{max} on ^{18}F-NaF PET/CT (1.35±0.21 versus 1.07±0.27, respectively; *P*=0.0030; Figure 3). Table 2 shows case information and individual CCTA and ^{18}F-NaF PET/CT findings in culprit lesions. Note that all 4 culprit lesions without obstructive stenosis on CCTA had TBR_{max} ≥1.28 on ^{18}F-NaF PET/CT; 5 culprit lesions did not correspond with M-TBR_{max}. Figures 4 through 6 show representative cases.

CCTA Findings and Higher M-TBR_{max}

To investigate the effective combination of CCTA and ^{18}F-NaF PET/CT, we performed patient- and lesion-based analyses of the relationship between CCTA findings and the presence of TBR_{max} ≥1.28 in the entire cohort.

Among all 41 patients, 14 (34%) had M-TBR_{max} ≥1.28 on ^{18}F-NaF PET/CT. Among the 31 patients without coronary stents in whom CCS could be measured, those with M-TBR_{max} ≥1.28 (n=11) had higher CCS than those with M-TBR_{max} <1.28 (573 [interquartile range: 207–2182] versus 143 [interquartile range: 19–530], respectively; *P*=0.043; Figure 7A). A higher percentage of patients with M-TBR_{max} ≥1.28 than of those with lower M-TBR_{max} had at least 1 HRP on CCTA (86% versus 52% of patients, respectively; *P*=0.033; Figure 7B); this group also had more HRPs per patient (1.2±0.8 versus 0.7±0.7, respectively; *P*=0.034). However, there was no difference between the groups in the frequency of obstructive stenosis on CCTA (64% versus 59%, respectively; *P*=0.75; Figure 7C). On multivariate analysis adjusted for age, sex, presence of coronary risk factors, and statin use, the presence of HRP on CCTA remained a significant predictor

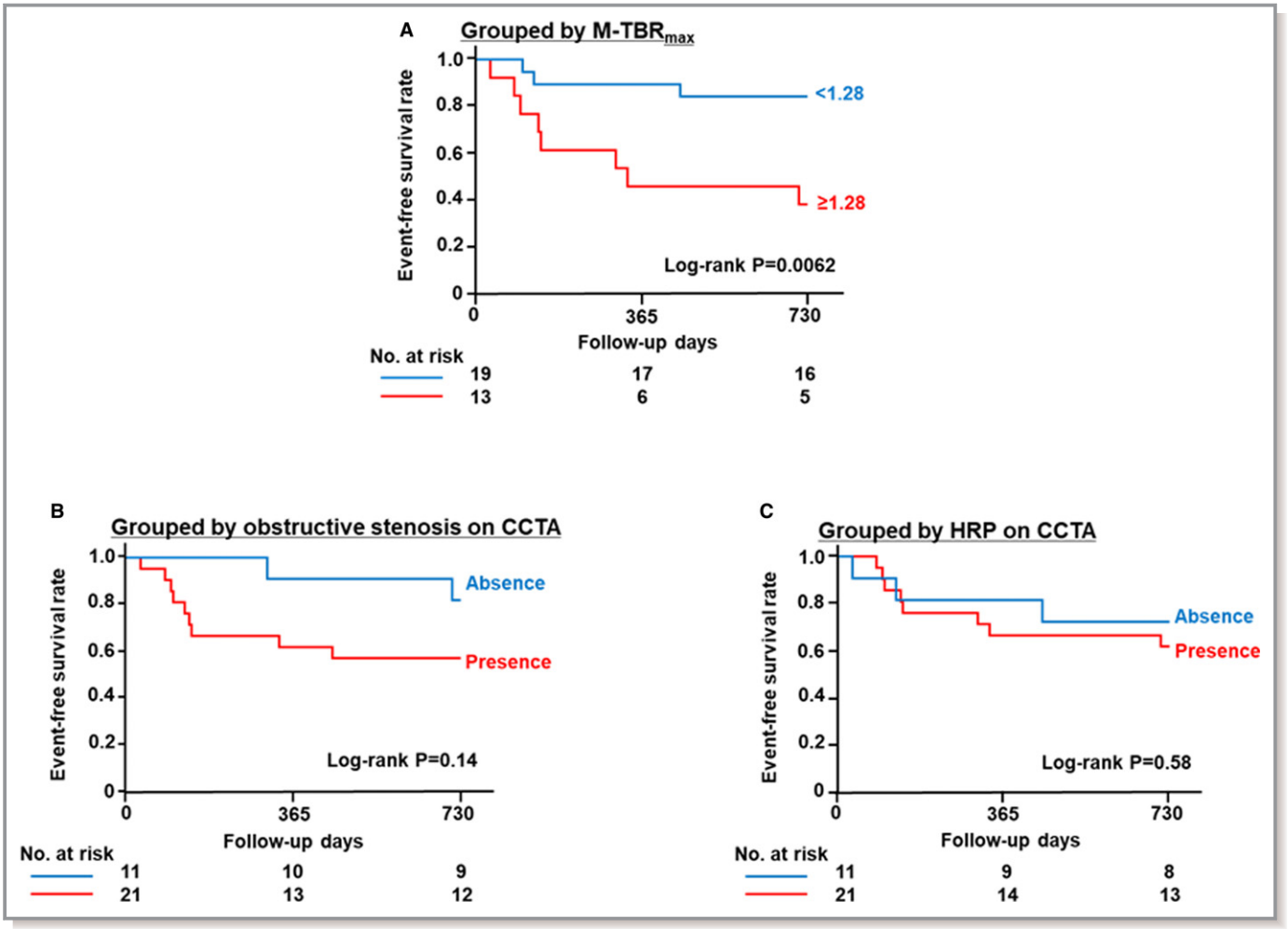

Figure 2. Kaplan–Meier curves for coronary events stratified according to patient-based ^{18}F-sodium fluoride (^{18}F-NaF) TBR$_{max}$ (A), presence or absence of obstructive stenosis on CCTA (B), and presence or absence of HRP on CCTA (C). Patients with maximum TBR$_{max}$ ≥1.28 in any coronary atherosclerotic lesion (M-TBR$_{max}$) had poorer outcomes than those with lower values (*P*=0.0062 by log-rank test) (A). Patients with obstructive coronary stenosis (*P*=0.14) (B) and those with HRP (*P*=0.58) (C) did not have poorer outcomes than patients without those findings. CCTA indicates coronary computed tomography angiography; HRP, high-risk plaque; TBR$_{max}$, maximum tissue:background ratio.

of M-TBR$_{max}$ ≥1.28 on ^{18}F-NaF PET/CT (odds ratio: 10.3; 95% CI, 1.8–99.5; *P*=0.0081; Table S2).

Among all 143 lesions, 25 (17%) had TBR$_{max}$ ≥1.28 on ^{18}F-NaF PET/CT. A higher percentage of lesions with TBR$_{max}$ ≥1.28 than of those with lower TBR$_{max}$ were classified as PCP (68% versus 36% of lesions, respectively; *P*=0.0028; Figure 8A) and HRP (48% versus 19%, respectively; *P*=0.0026; Figure 8B) on CCTA. There was no difference between lesions with TBR$_{max}$ ≥1.28 versus <1.28 in the frequency of obstructive stenosis on CCTA (36% versus 30% of lesions, respectively; *P*=0.53; Figure 8C). On multivariate analysis adjusted for lesion location (left main coronary artery, left anterior descending artery, left circumflex artery, or right coronary artery) and presence of obstructive stenosis on CCTA, plaque characterization as PCP (odds ratio: 3.4; 95% CI, 1.4–9.3; *P*=0.0082) and HRP (odds ratio: 3.6; 95% CI, 1.4–9.5; *P*=0.0098) on CCTA remained significant predictors of TBR$_{max}$ ≥1.28 on ^{18}F-NaF PET/CT.

Discussion

Our findings demonstrate that higher coronary ^{18}F-NaF uptake per patient has a predictive value for 2-year coronary events. To the best of our knowledge, this study is the first to report the prognostic value of ^{18}F-NaF PET/CT and its superiority to that of CCTA in the management of CAD. We found that higher coronary ^{18}F-NaF uptake per patient correlated with advanced coronary calcium and that the presence of HRP on CCTA was a predictor of higher coronary ^{18}F-NaF uptake in both patient- and lesion-based analyses. Despite the small cohort, our current results provide data to enhance the application of ^{18}F-NaF PET/CT to the

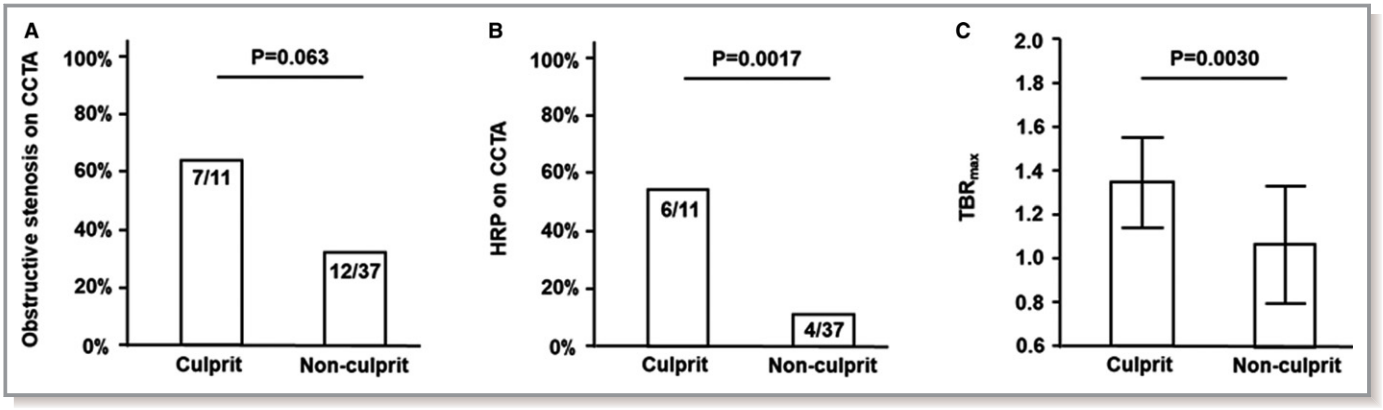

Figure 3. Prevalence of obstructive stenosis (A) and HRP (B) on CCTA, and ^{18}F-sodium fluoride (^{18}F-NaF) TBR_{max} in culprit vs nonculprit lesions in patients with coronary events. In the culprit lesions, obstructive stenosis was more likely to be observed (A), HRP was observed more frequently (B), and ^{18}F-NaF TBR_{max} was significantly higher (C) than in nonculprit lesions. CCTA indicates coronary computed tomography angiography; HRP, high-risk plaque; TBR_{max}, maximum tissue:background ratio.

management of CAD and support the implementation of a step-by-step approach using CCTA and ^{18}F-NaF PET/CT for noninvasive identification of high-risk CAD.

Prognostic Significance of ^{18}F-NaF PET/CT Versus CCTA

Noninvasive identification of CAD at high-risk for future coronary events is strongly desired. CCTA is promising and has been widely used as a noninvasive tool for assessing coronary atherosclerosis; however, CCTA-based high-risk features of coronary plaque have high prevalence and low positive predictive value for clinical events. A recent large cohort study found that detection of a high-risk plaque on CCTA had limited prognostic value among individuals with stable CAD.[17] Notably, only 6.4% of patients with high-risk coronary plaques in that study developed major adverse cardiovascular events during a median follow-up of 25 months. Thus, there is a need for a new and additive imaging modality to increase the accuracy of detecting "true" high-risk CAD.

In the current study, ^{18}F-NaF uptake showed promising potential as a method of predicting future coronary events, beyond coronary plaque analysis with CCTA. Whereas CCTA roughly assesses morphology, such as outward remodeling, of coronary atherosclerosis and plaque components, ^{18}F-NaF uptake reflects metabolically active coronary lesions with ongoing calcifying activity and vascular inflammation. We

Table 2. Case Information and Findings on CCTA and ^{18}F-NaF PET/CT in Culprit Lesions of Coronary Events

					CCTA		^{18}F-NaF PET/CT	
Patient Number	Age, y	Sex	End Point	Interval (d)	Obstructive Stenosis	HRP	≥1.28 TBR_{max}	Corresponding to M-TBR_{max}
1	65	Male	MI	450	Yes	No	No	No
2	59	Female	UA	138	No	No	Yes	Yes
3	66	Male	UA	85	No	Yes	Yes	No
4	72	Male	UA	32	Yes	No	Yes	Yes
5	62	Male	CR	128	Yes	No	No	No
6	80	Male	CR	711	No	Yes	Yes	Yes
7	73	Male	CR	143	Yes	Yes	Yes	No
8	70	Male	CR	334	Yes	Yes	Yes	Yes
9	78	Male	CR	103	Yes	No	No	No
10	68	Male	CR	98	Yes	Yes	Yes	Yes
11	63	Male	CR	308	No	Yes	Yes	Yes

^{18}F-NaF indicates ^{18}F-sodium fluoride; CCTA, coronary computed tomography angiography; CR, coronary revascularization; CT, computed tomography; HRP, high-risk plaque; MI, myocardial infarction; M-TBR_{max}, maximum TBR_{max} per patient; PET, positron emission tomography; TBR_{max}, maximum tissue:background ratio; UA, unstable angina.

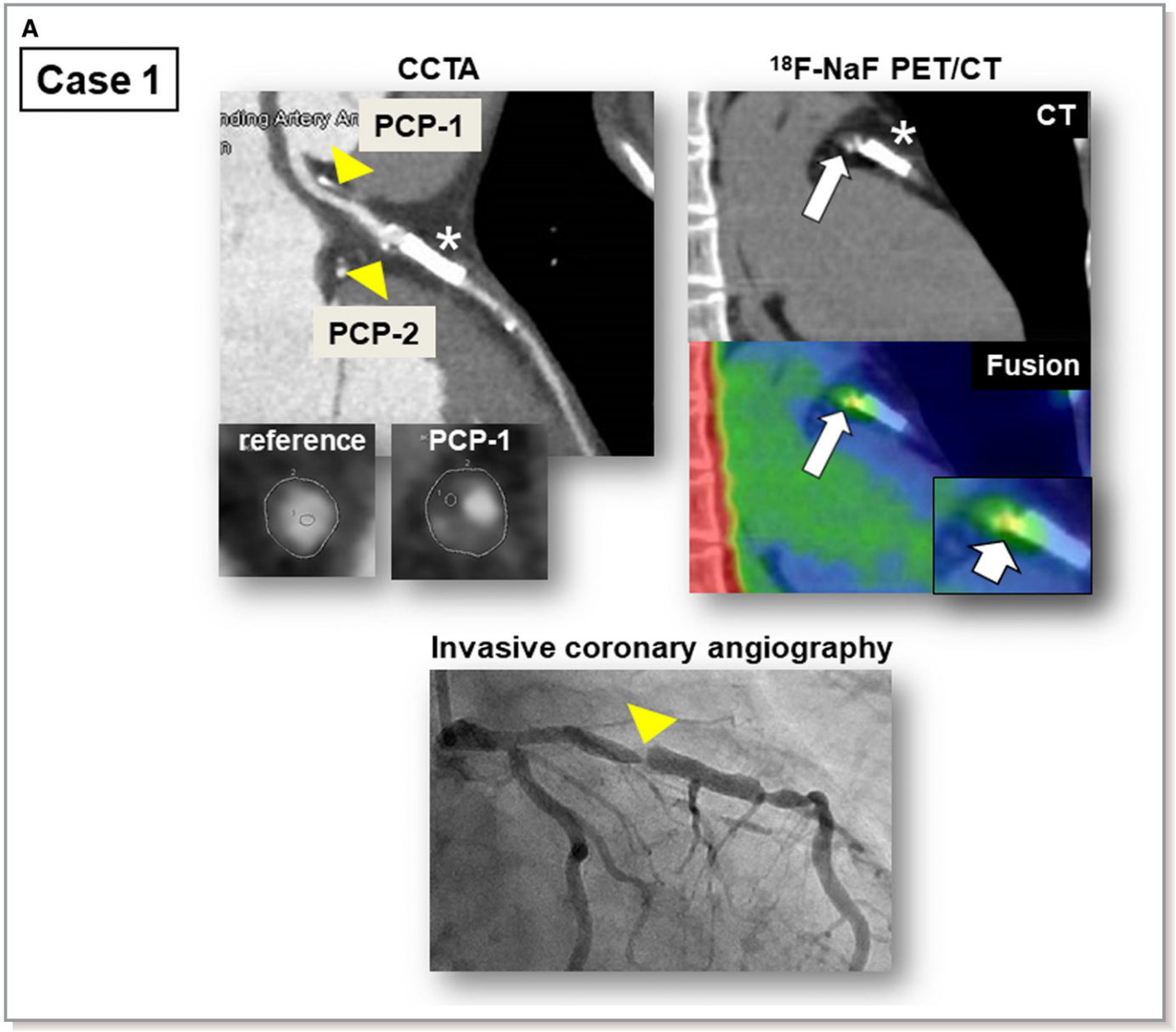

Figure 4. Representative cases showing relationship between ^{18}F-sodium fluoride (^{18}F-NaF) PET/CT findings and occurrence of coronary events. In case 1 (A), CCTA revealed a PCP and nonobstructive stenosis (50–69% at PCP-1) in the proximal portion of the left anterior descending artery (CCTA, arrowheads). PCP-1 was defined as an HRP (minimum CT density: 13 HU; remodeling index: 1.24). The fused PET/CT image showed enhanced ^{18}F-NaF uptake corresponding to PCP-2 (TBR_{max}: 1.6; ^{18}F-NaF PET/CT, arrows). Four months after ^{18}F-NaF PET/CT scan, this patient experienced unstable angina resulting from subtotal occlusion in the lesion corresponding to PCP-2 (invasive coronary angiography, arrow). In case 2 (B), CCTA revealed PCP, defined as HRP (minimum CT density: 25 HU; remodeling index: 1.50), and obstructive stenosis (≥70%) in the proximal portion of the left anterior descending artery (CCTA, arrowhead). The fused PET/CT image showed minimal ^{18}F-NaF uptake (TBR_{max}: 1.0) corresponding to the PCP (^{18}F-NaF PET/CT, arrows). This patient had no coronary event during the follow-up period. Asterisk indicates implanted coronary stent. CCTA indicates coronary computed tomography angiography; CT, computed tomography; HRP, high-risk plaque; HU, Hounsfield units; PCP, partially calcified plaque; PET, positron emission tomography; TBR_{max}, maximum tissue: background ratio.

found that patient-based ^{18}F-NaF accumulation in any coronary lesion had a prognostic value for the prediction of combined coronary events. High ^{18}F-NaF uptake in any lesion in the entire coronary tree may be significant in risk stratification for individual patients, suggesting the importance of systemic assessment of coronary atherosclerosis. This concept is supported by our finding that almost half (5/11) of the culprit lesions for coronary events did not have

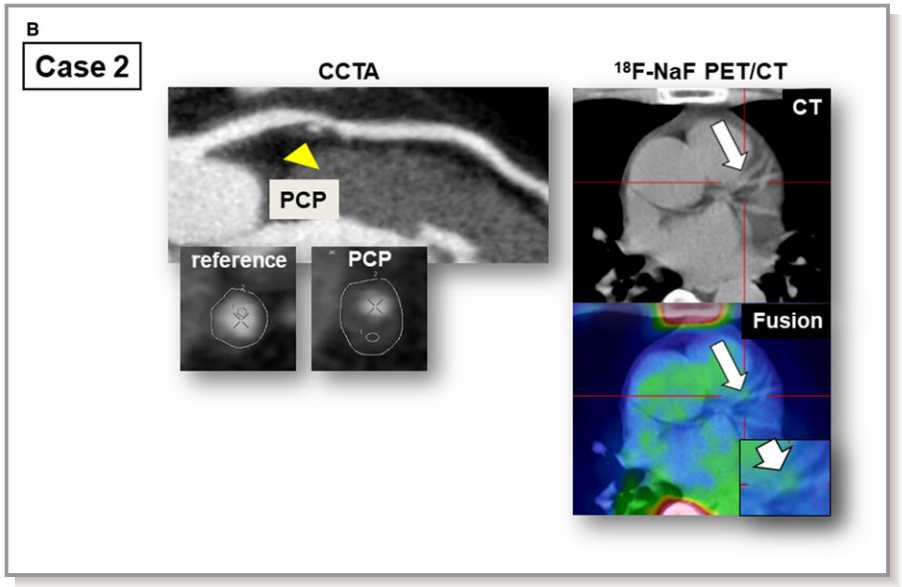

Figure 4. Continued

maximum ^{18}F-NaF accumulation. We found that the culprit lesions had higher ^{18}F-NaF uptake than nonculprit lesions. We identified the optimal cutoff for patient-based maximum TBR_{max} to be 1.28 for predicting future coronary events; almost all culprit lesions both for ACS (3/4) and late coronary revascularization (5/7) had an individual TBR_{max}

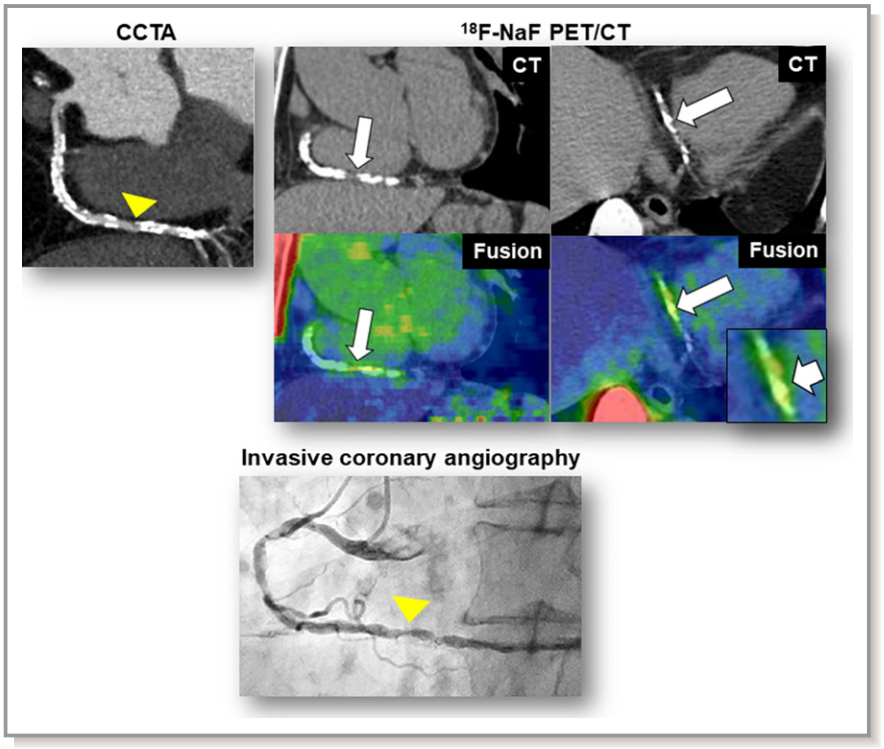

Figure 5. Additional representative case 1. CCTA revealed heavy coronary calcification and obstructive stenosis (≥70%) in the distal portion of the right coronary artery (CCTA, arrowhead). The fused PET/CT images showed enhanced ^{18}F-sodium fluoride (^{18}F-NaF) uptake corresponding to the calcification (maximum tissue-to-background ratio=1.6) (^{18}F-NaF PET/CT, arrows). This patient experienced unstable angina resulting from subtotal occlusion in the lesion corresponding to the calcification (invasive coronary angiography, arrow) 1 month after ^{18}F-NaF PET/CT scan. CCTA indicates coronary computed tomography angiography; CT, computed tomography; PET, positron emission tomography.

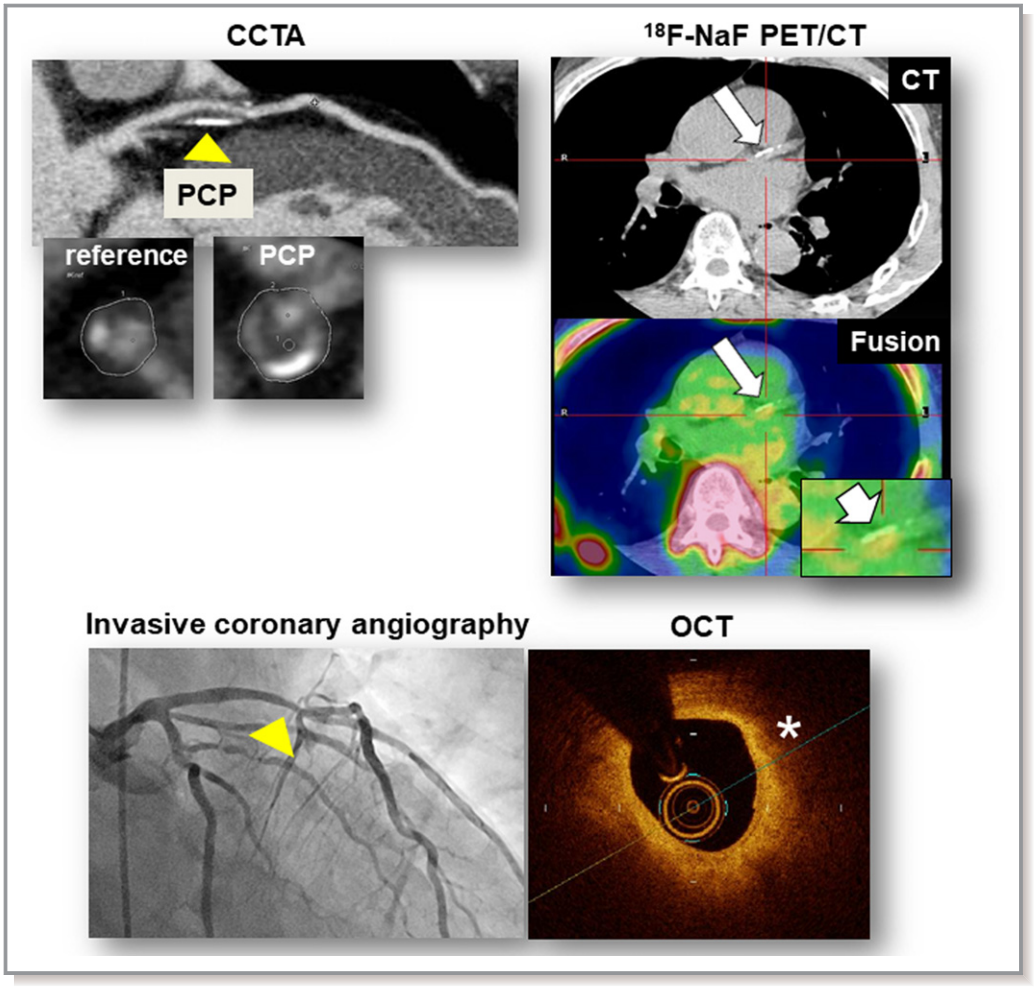

Figure 6. Additional representative case 2. CCTA revealed PCP, defined as a high-risk plaque (minimum CT density: 20 HU; remodeling index: 1.38), and nonobstructive stenosis (50–69%) in the proximal portion of the left anterior descending artery (CCTA, arrowheads). The fused PET/CT image showed enhanced ^{18}F-sodium fluoride (^{18}F-NaF) uptake corresponding to the PCP (TBR_{max}: 1.33; ^{18}F-NaF PET/CT, arrows). This patient underwent coronary revascularization of the lesion corresponding to the PCP (invasive coronary angiography, arrow) 23 months after ^{18}F-NaF PET/CT scan because of chest pain and impaired coronary fractional flow reserve (0.73). OCT showed the lipid-rich characteristic of the lesions corresponding to the PCP (OCT, asterisk). CCTA indicates coronary computed tomography angiography; CT, computed tomography; HU, Hounsfield units; OCT, optical coherence tomography; PCP, partially calcified plaque; PET, positron emission tomography; TBR_{max}, maximum tissue:background ratio.

equal to or above the cutoff. Despite the low sensitivity and specificity of the cutoff, it may be a useful indicator in screening for high-risk patients and coronary lesions.

The presence of obstructive stenosis on CCTA appears to have significance for the prediction of coronary events. In a midterm (mean: 3.9 years) follow-up study of CCTA, patients with marked stenosis (≥70%) had a higher rate of ACS than other patients.[18] In our study, most enrolled patients had obstructive stenosis on CCTA, which may in part reflect the general trend of overestimation of coronary stenosis on CCTA. In patients with known or suspected CAD, the assessment of coronary stenosis on CCTA may have limited specificity in CAD risk stratification. Notably, the 2 culprit lesions in this study that caused MI or UA without obstructive stenosis on CCTA had enhanced ^{18}F-NaF uptake (TBR_{max} ≥1.28), indicating the novel usefulness of ^{18}F-NaF PET/CT in CAD risk assessment (case 2 in Figure 4).

Combining CCTA and ^{18}F-NaF PET

According to our follow-up study, predicting enhanced ^{18}F-NaF uptake in coronary atherosclerosis is important. Because it is not practical to perform ^{18}F-NaF PET/CT in the general population, criteria are needed for identifying patients in whom the procedure could be beneficial. In an early report on coronary ^{18}F-NaF PET/CT,[1] ^{18}F-NaF uptake in coronary

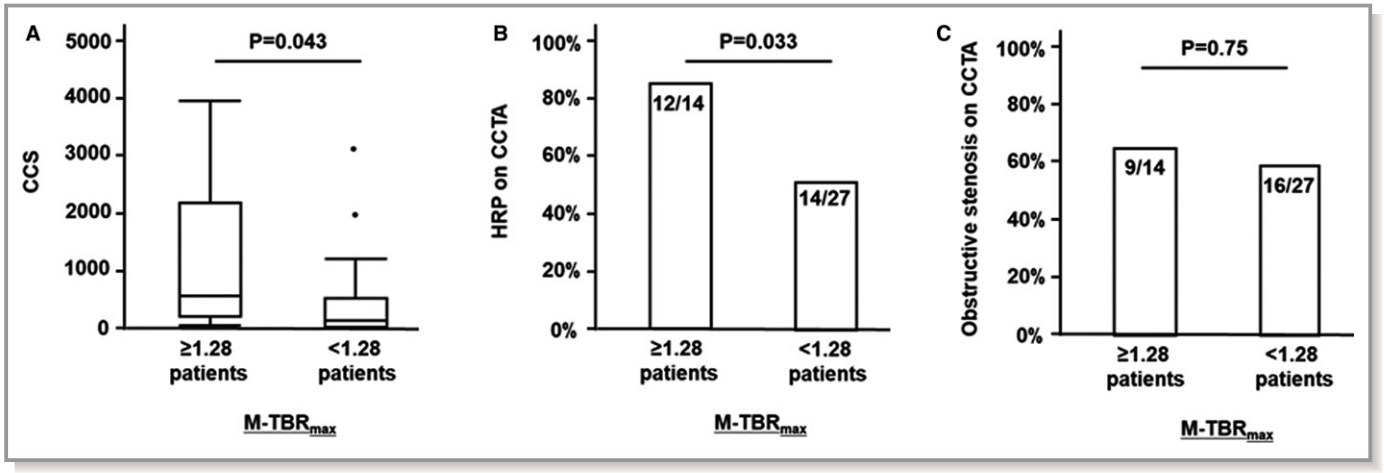

Figure 7. CCS (A) and prevalence of HRP (B) and obstructive stenosis (C) on CCTA according to patient-based ^{18}F-sodium fluoride (^{18}F-NaF) TBR_{max}. Patients with maximum TBR_{max} ≥1.28 in any coronary atherosclerotic lesion (M-TBR_{max}) had higher CCS (A) and a higher prevalence of at least 1 HRP (B) than those with lower values. A prevalence of obstructive coronary stenosis was similar between the groups (C). CCS indicates coronary calcium score; CCTA, coronary computed tomography angiography; CT, computed tomography; HRP, high-risk plaque; PCP, partially calcified plaque; PET, positron emission tomography; TBR_{max}, maximum tissue:background ratio.

arteries increased as CCS increased. Another recent study demonstrated that coronary plaques with high-risk characteristics on intravascular imaging (intravascular ultrasound and optical coherence tomography) had higher ^{18}F-NaF TBR than those without such characteristics.[19] In that study, the prevalence of adverse plaque characteristics on CCTA (low attenuation, positive remodeling, napkin-ring sign, and spotty calcification) was not different between ^{18}F-NaF-positive (>25% higher uptake than reference lesion) and ^{18}F-NaF–negative plaques; however, plaque burden and remodeling index were higher in ^{18}F-NaF–positive plaques. In human carotid plaques, associations have also been reported between high-risk characteristics on CT (plaque burden and positive remodeling) and ^{18}F-NaF uptake.[20] Thus, coronary atherosclerosis burden and high-risk coronary plaques, which may be substantially assessed with cardiac CT, appear to be associated with ^{18}F-NaF accumulation.

In this study, we investigated which CCTA findings predicted ^{18}F-NaF TBR_{max} equal to or above the cutoff (1.28). Patient-based analysis demonstrated that higher CCS and the presence of HRP on CCTA were associated with coronary ^{18}F-NaF TBR_{max} equal to or above the cutoff, whereas the presence of obstructive stenosis was not. In lesion-based analysis, the findings of PCP and HRP on CCTA strongly correlated with individual ^{18}F-NaF TBR_{max} equal to or above the cutoff. Our results suggest that ^{18}F-NaF

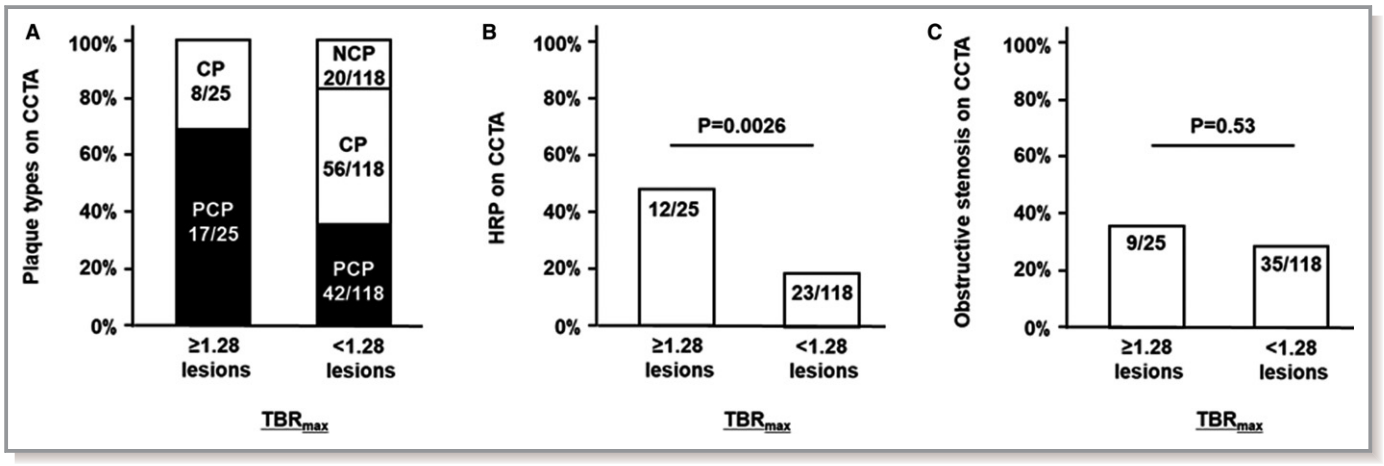

Figure 8. Distribution of plaque types, prevalence of HRP, and prevalence of obstructive stenosis on CCTA according to lesion-based ^{18}F-sodium fluoride (^{18}F-NaF) TBR_{max}. Coronary atherosclerotic lesions with TBR_{max} ≥1.28 were more frequently defined as PCP (A) and HRP (B) than those with lower values on CCTA. A prevalence of obstructive coronary stenosis was similar between the groups (C). CCTA indicates coronary computed tomography angiography; CP, calcified plaque; CT, computed tomography; HRP, high-risk plaque; NCP, noncalcified plaque; PCP, partially calcified plaque; PET, positron emission tomography; TBR_{max}, maximum tissue:background ratio.

accumulation in CAD may be related not only to the quantitative progression of coronary atherosclerosis (CCS) but also to its biological state. This means that coronary calcification in heterogeneous plaques (PCP, HRP) is likely to be metabolically active.

Compared with intravascular ultrasound and optical coherence tomography, CCTA has advantages in the noninvasive approach to CAD. Our results suggest the usefulness of CCTA in identifying CAD and coronary lesions that are likely to have enhanced ^{18}F-NaF uptake. Patients with higher CCS and/or HRP on CCTA could be suitable for ^{18}F-NaF PET/CT examination. In the assessment of ^{18}F-NaF PET/CT images, we should focus on ^{18}F-NaF uptake especially in PCP and HRP. These ideas are helpful for the step-by-step utilization of CCTA and ^{18}F-NaF PET/CT in CAD risk stratification.

Limitations

We acknowledge some limitations of this study. First, the sample size was small, and we found low post hoc study powers for our nonsignificant results (eg, differences in CCTA findings between groups). Because of the small cohort, we could not statistically investigate ^{18}F-NaF uptake for hard coronary events (cardiac death and ACS) alone. The prediction of hard coronary events is clinically important and should be investigated with ^{18}F-NaF PET/CT or a combination of CCTA and ^{18}F-NaF PET/CT in a larger cohort. Second, the heterogeneity of patients should be interpreted with caution. We included patients both with and without a history of CAD. Thus, our current results do not indicate the usefulness of ^{18}F-NaF PET/CT in the primary assessment of CAD. Third, the difficulty in merging the PET data with prior CCTA data and the lower spatial resolution of PET/CT images compared with CCTA images are technical limitations of our method. Using CCTA scanned at the time of PET/CT is recommended and future improvements in the spatial resolution of PET/CT images will promote our concept. Finally, we did not acquire histological information about coronary lesions with ^{18}F-NaF uptake. This aspect is worthy of future investigation in human samples or experimental animal models.

Conclusions

The results of this study suggest that ^{18}F-NaF PET/CT has the potential to detect high-risk CAD and individual coronary lesions and to predict future coronary events when combined with CCTA. Our study highlights the prognostic value of ^{18}F-NaF uptake in coronary arteries, which provides clinically meaningful information for the management of CAD. Further study in a larger cohort is warranted to clarify the clinical utility of this new imaging option.

Acknowledgments

We acknowledge the help and support of the radiography and radiochemistry staffs of the Hiroshima Heiwa Clinic. We also thank Rebecca Tollefson, DVM, from Edanz Group for editing a draft of this article.

Sources of Funding

This study was supported by a Japan Heart Foundation Research Grant, a Takeda Science Foundation Research Grant, and a JSPS KAKENHI Grant-in-Aid for Scientific Research (grant no. 17K09502).

Disclosures

None.

References

1. Dweck MR, Chow MW, Joshi NV, Williams MC, Jones C, Fletcher AM, Richardson H, White A, McKillop G, van Beek EJ, Boon NA, Rudd JH, Newby DE. Coronary arterial ^{18}F-sodium fluoride uptake: a novel marker of plaque biology. *J Am Coll Cardiol*. 2012;59:1539–1548.
2. Derlin T, Tóth Z, Papp L, Wisotzki C, Apostolova I, Habermann CR, Mester J, Klutmann S. Correlation of inflammation assessed by ^{18}F-FDG PET, active mineral deposition assessed by ^{18}F-fluoride PET, and vascular calcification in atherosclerotic plaque: a dual tracer PET/CT study. *J Nucl Med*. 2011;52:1020–1027.
3. Dweck MR, Jones C, Joshi NV, Fletcher AM, Richardson H, White A, Marsden M, Pessotto R, Clark JC, Wallace WA, Salter DM, McKillop G, van Beek EJ, Boon NA, Rudd JH, Newby DE. Assessment of valvular calcification and inflammation by positron emission tomography in patients with aortic stenosis. *Circulation*. 2012;125:76–86.
4. Aikawa E, Nahrendorf M, Figueiredo JL, Swirski FK, Shtatland T, Kohler RH, Jaffer FA, Aikawa M, Weissleder R. Osteogenesis associates with inflammation in early-stage atherosclerosis evaluated by molecular imaging in vivo. *Circulation*. 2007;116:2841–2850.
5. New SE, Goettsch C, Aikawa M, Marchini JF, Shibasaki M, Yabusaki K, Libby P, Shanahan CM, Croce K, Aikawa E. Macrophage-derived matrix vesicles: an alternative novel mechanism for microcalcification in atherosclerotic plaques. *Circ Res*. 2013;113:72–77.
6. Oliveira-Santos M, Castelo-Branco M, Silva R, Gomes A, Chichorro N, Abrunhosa A, Donato P, Pedroso de Lima J, Pego M, Gonçalves L, Ferreira MJ. Atherosclerotic plaque metabolism in high cardiovascular risk subjects—a subclinical atherosclerosis imaging study with ^{18}F-NaF PET-CT. *Atherosclerosis*. 2017;260:41–46.
7. Kitagawa T, Yamamoto H, Toshimitsu S, Sasaki K, Senoo A, Kubo Y, Tatsugami F, Awai K, Hirokawa Y, Kihara Y. ^{18}F-sodium fluoride positron emission tomography for molecular imaging of coronary atherosclerosis based on computed tomography analysis. *Atherosclerosis*. 2017;263:385–392.
8. Joshi NV, Vesey AT, Williams MC, Shah AS, Calvert PA, Craighead FH, Yeoh SE, Wallace W, Salter D, Fletcher AM, van Beek EJ, Flapan AD, Uren NG, Behan MW, Cruden NL, Mills NL, Fox KA, Rudd JH, Dweck MR, Newby DE. ^{18}F-fluoride positron emission tomography for identification of ruptured and high-risk coronary atherosclerotic plaques: a prospective clinical trial. *Lancet*. 2014;383:705–713.
9. Raff GL, Abidov A, Achenbach S, Berman DS, Boxt LM, Budoff MJ, Cheng V, DeFrance T, Hellinger JC, Karlsberg RP; Society of Cardiovascular Computed Tomography. SCCT guidelines for the interpretation and reporting of coronary computed tomographic angiography. *J Cardiovasc Comput Tomogr*. 2009;3:122–136.
10. Kitagawa T, Yamamoto H, Sentani K, Takahashi S, Tsushima H, Senoo A, Yasui W, Sueda T, Kihara Y. The relationship between inflammation and neoangiogenesis of epicardial adipose tissue and coronary atherosclerosis based on computed tomography analysis. *Atherosclerosis*. 2015;243:293–299.
11. Kitagawa T, Yamamoto H, Ohhashi N, Okimoto T, Horiguchi J, Hirai N, Ito K, Kohno N. Comprehensive evaluation of non-calcified coronary plaque characteristics

detected using 64-slice computed tomography in patients with proven or suspected coronary artery disease. *Am Heart J*. 2007;154:1191–1198.

12. Kitagawa T, Yamamoto H, Horiguchi J, Ohhashi N, Tadehara F, Shokawa T, Dohi Y, Kunita E, Utsunomiya H, Kohno N, Kihara Y. Characterization of noncalcified coronary plaques and identification of culprit lesions in patients with acute coronary syndrome by 64-slice computed tomography. *JACC Cardiovasc Imaging*. 2009;2:153–160.
13. Motoyama S, Kondo T, Sarai M, Sugiura A, Harigaya H, Sato T, Inoue K, Okumura M, Ishii J, Anno H, Virmani R, Ozaki Y, Hishida H, Narula J. Multislice computed tomographic characteristics of coronary lesions in acute coronary syndromes. *J Am Coll Cardiol*. 2007;50:319–326.
14. Motoyama S, Sarai M, Harigaya H, Anno H, Inoue K, Hara T, Naruse H, Ishii J, Hishida H, Wong ND, Virmani R, Kondo T, Ozaki Y, Narula J. Computed tomographic angiography characteristics of atherosclerotic plaques subsequently resulting in acute coronary syndrome. *J Am Coll Cardiol*. 2009;54:49–57.
15. Braunwald E, Antman EM, Beasley JW, Califf RM, Cheitlin MD, Hochman JS, Jones RH, Kereiakes D, Kupersmith J, Levin TN, Pepine CJ, Schaeffer JW, Smith EE III, Steward DE, Theroux P, Gibbons RJ, Alpert JS, Faxon DP, Fuster V, Gregoratos G, Hiratzka LF, Jacobs AK, Smith SC Jr; American College of Cardiology; American Heart Association. Committee on the Management of Patients With Unstable Angina. ACC/AHA guideline update for the management of patients with unstable angina and non-ST-segment elevation myocardial infarction—2002: summary article: a report of the American College of Cardiology/American Heart Association Task Force on Practice Guidelines (Committee on the Management of Patients With Unstable Angina). *Circulation*. 2002;106:1893–1900.
16. Thygesen K, Alpert JS, Jaffe AS, Simoons ML, Chaitman BR, White HD; Joint ESC/ACCF/AHA/WHF Task Force for Universal Definition of Myocardial Infarction; Authors/Task Force Members Chairpersons, Thygesen K, Alpert JS, White HD; Biomarker Subcommittee, Jaffe AS, Katus HA, Apple FS, Lindahl B, Morrow DA; ECG Subcommittee, Chaitman BR, Clemmensen PM, Johanson P, Hod H; Imaging Subcommittee, Underwood R, Bax JJ, Bonow JJ, Pinto F, Gibbons RJ; Classification Subcommittee, Fox KA, Atar D, Newby LK, Galvani M, Hamm CW; Intervention Subcommittee, Uretsky BF, Steg PG, Wijns W, Bassand JP, Menasche P, Ravkilde J; Trials & Registries Subcommittee, Ohman EM, Antman EM, Wallentin LC, Armstrong PW, Simoons ML; Trials & Registries Subcommittee, Januzzi JL, Nieminen MS, Gheorghiade M, Filippatos G; Trials & Registries Subcommittee, Luepker RV, Fortmann SP, Rosamond WD, Levy D, Wood D; Trials & Registries Subcommittee, Smith SC, Hu D, Lopez-Sendon JL, Robertson RM, Weaver D, Tendera M, Bove AA, Parkhomenko AN, Vasilieva EJ, Mendis S; ESC Committee for Practice Guidelines (CPG), Bax JJ, Baumgartner H, Ceconi C, Dean V, Deaton C, Fagard R, Funck-Brentano C, Hasdai D, Hoes A, Kirchhof P, Knuuti J, Kolh P, McDonagh T, Moulin C, Popescu BA, Reiner Z, Sechtem U, Sirnes PA, Tendera M, Torbicki A, Vahanian A, Windecker S; Document Reviewers, Morais J, Aguiar C, Almahmeed W, Arnar DO, Barili F, Bloch KD, Bolger AF, Botker HE, Bozkurt B, Bugiardini R, Cannon C, de Lemos J, Eberli FR, Escobar E, Hlatky M, James S, Kern KB, Moliterno DJ, Mueller C, Neskovic AN, Pieske BM, Schulman SP, Storey RF, Taubert KA, Vranckx P, Wagner DR. Third universal definition of myocardial infarction. *J Am Coll Cardiol*. 2012;60:1581–1598.
17. Ferencik M, Mayrhofer T, Bittner DO, Emami H, Puchner SB, Lu MT, Meyersohn NM, Ivanov AV, Adami EC, Patel MR, Mark DB, Udelson JE, Lee KL, Douglas PS, Hoffmann U. Use of high-risk coronary atherosclerotic plaque detection for risk stratification of patients with stable chest pain: a secondary analysis of the PROMISE randomized clinical trial. *JAMA Cardiol*. 2018;3:144–152.
18. Motoyama S, Ito H, Sarai M, Kondo T, Kawai H, Nagahara Y, Harigaya H, Kan S, Anno H, Takahashi H, Naruse H, Ishii J, Hecht H, Shaw LJ, Ozaki Y, Narula J. Plaque characterization by coronary computed tomography angiography and the likelihood of acute coronary events in mid-term follow-up. *J Am Coll Cardiol*. 2015;66:337–346.
19. Lee JM, Bang JI, Koo BK, Hwang D, Park J, Zhang J, Yaliang T, Suh M, Paeng JC, Shiono Y, Kubo T, Akasaka T. Clinical relevance of ^{18}F-sodium fluoride positron-emission tomography in noninvasive identification of high-risk plaque in patients with coronary artery disease. *Circ Cardiovasc Imaging*. 2017;10:e006704.
20. Vesey AT, Jenkins WS, Irkle A, Moss A, Sng G, Forsythe RO, Clark T, Roberts G, Fletcher A, Lucatelli C, Rudd JH, Davenport AP, Mills NL, Al-Shahi Salman R, Dennis M, Whiteley WN, van Beek EJ, Dweck MR, Newby DE. ^{18}F-fluoride and ^{18}F-fluorodeoxyglucose positron emission tomography after transient ischemic attack or minor ischemic stroke: case-control study. *Circ Cardiovasc Imaging*. 2017;10:e004976.

SUPPLEMENTAL MATERIAL

Table S1. Multivariate Analysis of CCTA findings and ^{18}F-NaF Uptake in Predicting Coronary Events.

	Model 1	P value	Model 2	P value	Model 3	P value	Model 4	P value
Obstructive stenosis	3.0 (0.8 to 19.9)	0.12	3.5 (0.9 to 23.4)	0.076	5.4 (1.2 to 39.3)	0.025	9.4 (1.5 to 118.4)	0.014
HRP	1.4 (0.4 to 6.6)	0.57	1.3 (0.4 to 6.2)	0.65	1.6 (0.4 to 8.6)	0.55	1.0 (0.1 to 9.2)	0.97
≥1.28 M-TBR_{max}	5.3 (1.5 to 24.3)	0.0082	4.5 (1.2 to 23.1)	0.028	5.0 (1.1 to 30.8)	0.037	8.2 (1.4 to 79.2)	0.020

Data are expressed as hazard ratio (95% confidence interval).

Model 1: unadjusted

Model 2: adjusted for age, sex

Model 3: adjusted for age, sex, coronary risk factor, statin use

Model 4: adjusted for age, sex, coronary risk factor, statin use, obstructive stenosis, HRP, M-TBR_{max} ≥1.28

^{18}F-NaF, ^{18}F-sodium fluoride; CCTA, coronary computed tomography angiography; HRP, high-risk plaque; M-TBR_{max}, maximum TBR_{max} per patient; TBR_{max}, maximum tissue-to-background ratio.

Table S2. Multivariate Analysis of CCTA findings in Predicting Higher ^{18}F-NaF Uptake (M-TBR$_{max}$ ≥1.28).

	Model 1	P value	Model 2	P value	Model 3	P value	Model 4	P value
Obstructive stenosis	1.2 (0.3 to 5.0)	0.75	1.3 (0.3 to 5.3)	0.74	1.1 (0.3 to 4.9)	0.90	0.9 (0.2 to 4.8)	0.87
HRP	5.6 (1.2 to 40.4)	0.026	5.9 (1.2 to 44.1)	0.024	10.2 (1.7 to 99.6)	0.0082	10.3 (1.8 to 99.5)	0.0081

Data are expressed as odds ratio (95% confidence interval).

Model 1: unadjusted

Model 2: adjusted for age, sex

Model 3: adjusted for age, sex, coronary risk factor, statin use

Model 4: adjusted for age, sex, coronary risk factor, statin use, obstructive stenosis, HRP

^{18}F-NaF, ^{18}F-sodium fluoride; CCTA, coronary computed tomography angiography; HRP, high-risk plaque; M-TBR_{max}, maximum TBR_{max} per patient; TBR_{max}, maximum tissue-to-background ratio.